Midrapidity antiproton-to-proton ratio in pp collisions at $\sqrt{s} = 0.9$ and 7 TeV measured by the ALICE experiment

(The ALICE Collaboration)

K. Aamodt,[1] N. Abel,[2] U. Abeysekara,[3] A. Abrahantes Quintana,[4] A. Abramyan,[5] D. Adamová,[6] M.M. Aggarwal,[7] G. Aglieri Rinella,[8] A.G. Agocs,[9] S. Aguilar Salazar,[10] Z. Ahammed,[11] A. Ahmad,[12] N. Ahmad,[12] S.U. Ahn,[13,a] R. Akimoto,[14] A. Akindinov,[15] D. Aleksandrov,[16] B. Alessandro,[17] R. Alfaro Molina,[10] A. Alici,[18] E. Almaráz Aviña,[10] J. Alme,[19] T. Alt,[2,b] V. Altini,[20] S. Altinpinar,[21] C. Andrei,[22] A. Andronic,[21] G. Anelli,[8] V. Angelov,[2,b] C. Anson,[23] T. Antičić,[24] F. Antinori,[8,c] S. Antinori,[18] K. Antipin,[25] D. Antończyk,[25] P. Antonioli,[26] A. Anzo,[10] L. Aphecetche,[27] H. Appelshäuser,[25] S. Arcelli,[18] R. Arceo,[10] A. Arend,[25] N. Armesto,[28] R. Arnaldi,[17] T. Aronsson,[29] I.C. Arsene,[1,d] A. Asryan,[30] A. Augustinus,[8] R. Averbeck,[21] T.C. Awes,[31] J. Äystö,[32] M.D. Azmi,[12] S. Bablok,[19] M. Bach,[33] A. Badalà,[34] Y.W. Baek,[13,a] S. Bagnasco,[17] R. Bailhache,[21,e] R. Bala,[35] A. Baldisseri,[36] A. Baldit,[37] J. Bán,[38] R. Barbera,[39] G.G. Barnaföldi,[9] L. Barnby,[40] V. Barret,[37] J. Bartke,[41] F. Barile,[20] M. Basile,[18] V. Basmanov,[42] N. Bastid,[37] B. Bathen,[43] G. Batigne,[27] B. Batyunya,[44] C. Baumann,[43,e] I.G. Bearden,[45] B. Becker,[46,f] I. Belikov,[47] R. Bellwied,[48] E. Belmont-Moreno,[10] A. Belogianni,[49] L. Benhabib,[27] S. Beole,[35] I. Berceanu,[22] A. Bercuci,[21,g] E. Berdermann,[21] Y. Berdnikov,[50] L. Betev,[8] A. Bhasin,[51] A.K. Bhati,[7] L. Bianchi,[35] N. Bianchi,[52] C. Bianchin,[53] J. Bielčík,[54] J. Bielčíková,[6] A. Bilandzic,[55] L. Bimbot,[56] E. Biolcati,[35] A. Blanc,[37] F. Blanco,[39,h] F. Blanco,[57] D. Blau,[16] C. Blume,[25] M. Boccioli,[8] N. Bock,[23] A. Bogdanov,[58] H. Bøggild,[45] M. Bogolyubsky,[59] J. Bohm,[60] L. Boldizsár,[9] M. Bombara,[61] C. Bombonati,[53,i] M. Bondila,[32] H. Borel,[36] A. Borisov,[62] C. Bortolin,[53,j] S. Bose,[63] L. Bosisio,[64] F. Bossú,[35] M. Botje,[55] S. Böttger,[2] G. Bourdaud,[27] B. Boyer,[56] M. Braun,[30] P. Braun-Munzinger,[21,65,b] L. Bravina,[1] M. Bregant,[64,k] T. Breitner,[2] G. Bruckner,[8] R. Brun,[8] E. Bruna,[29] G.E. Bruno,[20] D. Budnikov,[42] H. Buesching,[25] P. Buncic,[8] O. Busch,[66] Z. Buthelezi,[67] D. Caffarri,[53] X. Cai,[68] H. Caines,[29] E. Camacho,[69] P. Camerini,[64] M. Campbell,[8] V. Canoa Roman,[8] G.P. Capitani,[52] G. Cara Romeo,[26] F. Carena,[8] W. Carena,[8] F. Carminati,[8] A. Casanova Díaz,[52] M. Caselle,[8] J. Castillo Castellanos,[36] J.F. Castillo Hernandez,[21] V. Catanescu,[22] E. Cattaruzza,[64] C. Cavicchioli,[8] P. Cerello,[17] V. Chambert,[56] B. Chang,[60] S. Chapeland,[8] A. Charpy,[56] J.L. Charvet,[36] S. Chattopadhyay,[63] S. Chattopadhyay,[11] M. Cherney,[3] C. Cheshkov,[8] B. Cheynis,[70] E. Chiavassa,[35] V. Chibante Barroso,[8] D.D. Chinellato,[71] P. Chochula,[8] K. Choi,[72] M. Chojnacki,[73] P. Christakoglou,[73] C.H. Christensen,[45] P. Christiansen,[74] T. Chujo,[75] F. Chuman,[76] C. Cicalo,[46] L. Cifarelli,[18] F. Cindolo,[26] J. Cleymans,[67] O. Cobanoglu,[35] J.-P. Coffin,[47] S. Coli,[17] A. Colla,[8] G. Conesa Balbastre,[52] Z. Conesa del Valle,[27,l] E.S. Conner,[77] P. Constantin,[66] G. Contin,[64,i] J.G. Contreras,[69] Y. Corrales Morales,[35] T.M. Cormier,[48] P. Cortese,[78] I. Cortés Maldonado,[79] M.R. Cosentino,[71] F. Costa,[8] M.E. Cotallo,[57] E. Crescio,[69] P. Crochet,[37] E. Cuautle,[80] L. Cunqueiro,[52] J. Cussonneau,[27] A. Dainese,[81] H.H. Dalsgaard,[45] A. Danu,[82] I. Das,[63] A. Dash,[83] S. Dash,[83] G.O.V. de Barros,[84] A. De Caro,[85] G. de Cataldo,[86] J. de Cuveland,[2,b] A. De Falco,[87] M. De Gaspari,[66] J. de Groot,[8] D. De Gruttola,[85] N. De Marco,[17] S. De Pasquale,[85] R. De Remigis,[17] R. de Rooij,[73] G. de Vaux,[67] H. Delagrange,[27] G. Dellacasa,[78] A. Deloff,[88] V. Demanov,[42] E. Dénes,[9] A. Deppman,[84] G. D'Erasmo,[20] D. Derkach,[30] A. Devaux,[37] D. Di Bari,[20] C. Di Giglio,[20,i] S. Di Liberto,[89] A. Di Mauro,[8] P. Di Nezza,[52] M. Dialinas,[27] L. Díaz,[80] R. Díaz,[32] T. Dietel,[43] R. Divià,[8] Ø. Djuvsland,[19] V. Dobretsov,[16] A. Dobrin,[74] T. Dobrowolski,[88] B. Dönigus,[21] I. Domínguez,[80] D.M.M. Don,[90] O. Dordic,[1] A.K. Dubey,[11] J. Dubuisson,[8] L. Ducroux,[70] P. Dupieux,[37] A.K. Dutta Majumdar,[63] M.R. Dutta Majumdar,[11] D. Elia,[86] D. Emschermann,[66,m] A. Enokizono,[31] B. Espagnon,[56] M. Estienne,[27] S. Esumi,[75] D. Evans,[40] S. Evrard,[8] G. Eyyubova,[1] C.W. Fabjan,[8,n] D. Fabris,[81] J. Faivre,[91] D. Falchieri,[18] A. Fantoni,[52] M. Fasel,[21] O. Fateev,[44] R. Fearick,[67] A. Fedunov,[44] D. Fehlker,[19] V. Fekete,[92] D. Felea,[82] B. Fenton-Olsen,[45,o] G. Feofilov,[30] A. Fernández Téllez,[79] E.G. Ferreiro,[28] A. Ferretti,[35] R. Ferretti,[78,p] M.A.S. Figueredo,[84] S. Filchagin,[42] R. Fini,[86] F.M. Fionda,[20] E.M. Fiore,[20] M. Floris,[87,i] Z. Fodor,[9] S. Foertsch,[67] P. Foka,[21] S. Fokin,[16] F. Formenti,[8] E. Fragiacomo,[93] M. Fragkiadakis,[49] U. Frankenfeld,[21] A. Frolov,[94] U. Fuchs,[8] F. Furano,[8] C. Furget,[91] M. Fusco Girard,[85] J.J. Gaardhøje,[45] S. Gadrat,[91] M. Gagliardi,[35] A. Gago,[95] M. Gallio,[35] P. Ganoti,[49] M.S. Ganti,[11] C. Garabatos,[21] C. García Trapaga,[35] J. Gebelein,[2] R. Gemme,[78] M. Germain,[27] A. Gheata,[8] M. Gheata,[8] B. Ghidini,[20] P. Ghosh,[11] G. Giraudo,[17] P. Giubellino,[17] E. Gladysz-Dziadus,[41] R. Glasow,[43,q] P. Glässel,[66] A. Glenn,[96] R. Gómez Jiménez,[97] H. González Santos,[79] L.H. González-Trueba,[10] P. González-Zamora,[57] S. Gorbunov,[2,b] Y. Gorbunov,[3] S. Gotovac,[98] H. Gottschlag,[43] V. Grabski,[10] R. Grajcarek,[66] A. Grelli,[73] A. Grigoras,[8] C. Grigoras,[8] V. Grigoriev,[58]

A. Grigoryan,[5] S. Grigoryan,[44] B. Grinyov,[62] N. Grion,[93] P. Gros,[74] J.F. Grosse-Oetringhaus,[8] J.-Y. Grossiord,[70]
R. Grosso,[81] F. Guber,[99] R. Guernane,[91] B. Guerzoni,[18] K. Gulbrandsen,[45] H. Gulkanyan,[5] T. Gunji,[14]
A. Gupta,[51] R. Gupta,[51] H.-A. Gustafsson,[74,q] H. Gutbrod,[21] Ø. Haaland,[19] C. Hadjidakis,[56] M. Haiduc,[82]
H. Hamagaki,[14] G. Hamar,[9] J. Hamblen,[100] B.H. Han,[101] J.W. Harris,[29] M. Hartig,[25] A. Harutyunyan,[5] D. Hasch,[52]
D. Hasegan,[82] D. Hatzifotiadou,[26] A. Hayrapetyan,[5] M. Heide,[43] M. Heinz,[29] H. Helstrup,[102] A. Herghelegiu,[22]
C. Hernández,[21] G. Herrera Corral,[69] N. Herrmann,[66] K.F. Hetland,[102] B. Hicks,[29] A. Hiei,[76] P.T. Hille,[1,r]
B. Hippolyte,[47] T. Horaguchi,[76,s] Y. Hori,[14] P. Hristov,[8] I. Hřivnáčová,[56] S. Hu,[103] M. Huang,[19] S. Huber,[21]
T.J. Humanic,[23] D. Hutter,[33] D.S. Hwang,[101] R. Ichou,[27] R. Ilkaev,[42] I. Ilkiv,[88] M. Inaba,[75] P.G. Innocenti,[8]
M. Ippolitov,[16] M. Irfan,[12] C. Ivan,[73] A. Ivanov,[30] M. Ivanov,[21] V. Ivanov,[50] T. Iwasaki,[76] A. Jachołkowski,[8]
P. Jacobs,[104] L. Jančurová,[44] S. Jangal,[47] R. Janik,[92] C. Jena,[83] S. Jena,[105] L. Jirden,[8] G.T. Jones,[40] P.G. Jones,[40]
P. Jovanović,[40] H. Jung,[13] W. Jung,[13] A. Jusko,[40] A.B. Kaidalov,[15] S. Kalcher,[2,b] P. Kaliňák,[38] M. Kalisky,[43]
T. Kalliokoski,[32] A. Kalweit,[65] A. Kamal,[12] R. Kamermans,[73] K. Kanaki,[19] E. Kang,[13] J.H. Kang,[60] J. Kapitan,[6]
V. Kaplin,[58] S. Kapusta,[8] O. Karavichev,[99] T. Karavicheva,[99] E. Karpechev,[99] A. Kazantsev,[16] U. Kebschull,[2]
R. Keidel,[77] M.M. Khan,[12] S.A. Khan,[11] A. Khanzadeev,[50] Y. Kharlov,[59] D. Kikola,[106] B. Kileng,[102] D.J Kim,[32]
D.S. Kim,[13] D.W. Kim,[13] H.N. Kim,[13] J. Kim,[59] J.H. Kim,[101] J.S. Kim,[13] M. Kim,[13] M. Kim,[60] S.H. Kim,[13]
S. Kim,[101] Y. Kim,[60] S. Kirsch,[8] I. Kisel,[2,d] S. Kiselev,[15] A. Kisiel,[23,i] J.L. Klay,[107] J. Klein,[66] C. Klein-Bösing,[8,m]
M. Kliemant,[25] A. Klovning,[19] A. Kluge,[8] M.L. Knichel,[21] S. Kniege,[25] K. Koch,[66] R. Kolevatov,[1] A. Kolojvari,[30]
V. Kondratiev,[30] N. Kondratyeva,[58] A. Konevskih,[99] E. Kornaś,[41] R. Kour,[40] M. Kowalski,[41] S. Kox,[91]
K. Kozlov,[16] J. Kral,[54,k] I. Králik,[38] F. Kramer,[25] I. Kraus,[65,d] A. Kravčáková,[61] T. Krawutschke,[108] M. Krivda,[40]
D. Krumbhorn,[66] M. Krus,[54] E. Kryshen,[50] M. Krzewicki,[55] Y. Kucheriaev,[16] C. Kuhn,[47] P.G. Kuijer,[55] L. Kumar,[7]
N. Kumar,[7] R. Kupczak,[106] P. Kurashvili,[88] A. Kurepin,[99] A.N. Kurepin,[99] A. Kuryakin,[42] S. Kushpil,[6] V. Kushpil,[6]
M. Kutouski,[44] H. Kvaerno,[1] M.J. Kweon,[66] Y. Kwon,[60] P. La Rocca,[39,t] F. Lackner,[8] P. Ladrón de Guevara,[57]
V. Lafage,[56] C. Lal,[51] C. Lara,[2] D.T. Larsen,[19] G. Laurenti,[26] C. Lazzeroni,[40] Y. Le Bornec,[56] N. Le Bris,[27]
H. Lee,[72] K.S. Lee,[13] S.C. Lee,[13] F. Lefèvre,[27] M. Lenhardt,[27] L. Leistam,[8] J. Lehnert,[25] V. Lenti,[86] H. León,[10]
I. León Monzón,[97] H. León Vargas,[25] P. Lévai,[9] X. Li,[103] Y. Li,[103] R. Lietava,[40] S. Lindal,[1] V. Lindenstruth,[2,b]
C. Lippmann,[8] M.A. Lisa,[23] L. Liu,[19] V. Loginov,[58] S. Lohn,[8] X. Lopez,[37] M. López Noriega,[56] R. López-Ramírez,[79]
E. López Torres,[4] G. Løvhøiden,[1] A. Lozea Feijo Soares,[84] S. Lu,[103] M. Lunardon,[53] G. Luparello,[35] L. Luquin,[27]
J.-R. Lutz,[47] K. Ma,[68] R. Ma,[29] D.M. Madagodahettige-Don,[90] A. Maevskaya,[99] M. Mager,[65,i] D.P. Mahapatra,[83]
A. Maire,[47] I. Makhlyueva,[8] D. Mal'Kevich,[15] M. Malaev,[50] K.J. Malagalage,[3] I. Maldonado Cervantes,[80]
M. Malek,[56] T. Malkiewicz,[32] P. Malzacher,[21] A. Mamonov,[42] L. Manceau,[37] L. Mangotra,[51] V. Manko,[16]
F. Manso,[37] V. Manzari,[86] Y. Mao,[68,u] J. Mareš,[109] G.V. Margagliotti,[64] A. Margotti,[26] A. Marín,[21]
I. Martashvili,[100] P. Martinengo,[8] M.I. Martínez Hernández,[79] A. Martínez Davalos,[10] G. Martínez García,[27]
Y. Maruyama,[76] A. Marzari Chiesa,[35] S. Masciocchi,[21] M. Masera,[35] M. Masetti,[18] A. Masoni,[46] L. Massacrier,[70]
M. Mastromarco,[86] A. Mastroserio,[20,i] Z.L. Matthews,[40] A. Matyja,[41,v] D. Mayani,[80] G. Mazza,[17] M.A. Mazzoni,[89]
F. Meddi,[110] A. Menchaca-Rocha,[10] P. Mendez Lorenzo,[8] M. Meoni,[8] J. Mercado Pérez,[66] P. Mereu,[17] Y. Miake,[75]
A. Michalon,[47] N. Miftakhov,[50] L. Milano,[35] J. Milosevic,[1] F. Minafra,[20] A. Mischke,[73] D. Miśkowiec,[21] C. Mitu,[82]
K. Mizoguchi,[76] J. Mlynarz,[48] B. Mohanty,[11] L. Molnar,[9,i] M.M. Mondal,[11] L. Montaño Zetina,[69,w] M. Monteno,[17]
E. Montes,[57] M. Morando,[53] S. Moretto,[53] A. Morsch,[8] T. Moukhanova,[16] V. Muccifora,[52] E. Mudnic,[98]
S. Muhuri,[11] H. Müller,[8] M.G. Munhoz,[84] J. Munoz,[79] L. Musa,[8] A. Musso,[17] B.K. Nandi,[105] R. Nania,[26]
E. Nappi,[86] F. Navach,[20] S. Navin,[40] T.K. Nayak,[11] S. Nazarenko,[42] G. Nazarov,[42] A. Nedosekin,[15] F. Nendaz,[70]
J. Newby,[96] A. Nianine,[16] M. Nicassio,[86,i] B.S. Nielsen,[45] S. Nikolaev,[16] V. Nikolic,[24] S. Nikulin,[16] V. Nikulin,[50]
B.S. Nilsen,[3] M.S. Nilsson,[1] F. Noferini,[26] P. Nomokonov,[44] G. Nooren,[73] N. Novitzky,[32] A. Nyatha,[105]
C. Nygaard,[45] A. Nyiri,[1] J. Nystrand,[19] A. Ochirov,[30] G. Odyniec,[104] H. Oeschler,[65] M. Oinonen,[32] K. Okada,[14]
Y. Okada,[76] M. Oldenburg,[8] J. Oleniacz,[106] C. Oppedisano,[17] F. Orsini,[36] A. Ortiz Velasquez,[80] G. Ortona,[35]
A. Oskarsson,[74] F. Osmic,[8] L. Österman,[74] P. Ostrowski,[106] I. Otterlund,[74] J. Otwinowski,[21] G. Øvrebekk,[19]
K. Oyama,[66] K. Ozawa,[14] Y. Pachmayer,[66] M. Pachr,[54] F. Padilla,[35] P. Pagano,[85] G. Paić,[80] F. Painke,[2]
C. Pajares,[28] S. Pal,[63,x] S.K. Pal,[11] A. Palaha,[40] A. Palmeri,[34] R. Panse,[2] V. Papikyan,[5] G.S. Pappalardo,[34]
W.J. Park,[21] B. Pastirčák,[38] C. Pastore,[86] V. Paticchio,[86] A. Pavlinov,[48] T. Pawlak,[106] T. Peitzmann,[73]
A. Pepato,[81] H. Pereira,[36] D. Peressounko,[16] C. Pérez,[95] D. Perini,[8] D. Perrino,[20,i] W. Peryt,[106] J. Peschek,[2,b]
A. Pesci,[26] V. Peskov,[80,i] Y. Pestov,[94] A.J. Peters,[8] V. Petráček,[54] A. Petridis,[49,q] M. Petris,[22] P. Petrov,[40]
M. Petrovici,[22] C. Petta,[39] J. Peyré,[56] S. Piano,[93] A. Piccotti,[17] M. Pikna,[92] P. Pillot,[27] O. Pinazza,[26,i]

L. Pinsky,[90] N. Pitz,[25] F. Piuz,[8] R. Platt,[40] M. Płoskoń,[104] J. Pluta,[106] T. Pocheptsov,[44,y] S. Pochybova,[9]
P.L.M. Podesta Lerma,[97] F. Poggio,[35] M.G. Poghosyan,[35] K. Polák,[109] B. Polichtchouk,[59] P. Polozov,[15]
V. Polyakov,[50] B. Pommeresch,[19] A. Pop,[22] F. Posa,[20] V. Pospíšil,[54] B. Potukuchi,[51] J. Pouthas,[56] S.K. Prasad,[11]
R. Preghenella,[18,t] F. Prino,[17] C.A. Pruneau,[48] I. Pshenichnov,[99] G. Puddu,[87] P. Pujahari,[105] A. Pulvirenti,[39]
A. Punin,[42] V. Punin,[42] M. Putiš,[61] J. Putschke,[29] E. Quercigh,[8] A. Rachevski,[93] A. Rademakers,[8] S. Radomski,[66]
T.S. Räihä,[32] J. Rak,[32] A. Rakotozafindrabe,[36] L. Ramello,[78] A. Ramírez Reyes,[69] M. Rammler,[43]
R. Raniwala,[111] S. Raniwala,[111] S.S. Räsänen,[32] I. Rashevskaya,[93] S. Rath,[83] K.F. Read,[100] J.S. Real,[91]
K. Redlich,[88,z] R. Renfordt,[25] A.R. Reolon,[52] A. Reshetin,[99] F. Rettig,[2,b] J.-P. Revol,[8] K. Reygers,[43,aa]
H. Ricaud,[65] L. Riccati,[17] R.A. Ricci,[112] M. Richter,[19] P. Riedler,[8] W. Riegler,[8] F. Riggi,[39] A. Rivetti,[17]
M. Rodriguez Cahuantzi,[79] K. Røed,[102] D. Röhrich,[8,bb] S. Román López,[79] R. Romita,[20,d] F. Ronchetti,[52]
P. Rosinský,[8] P. Rosnet,[37] S. Rossegger,[8] A. Rossi,[64] F. Roukoutakis,[8,cc] S. Rousseau,[56] C. Roy,[27,l] P. Roy,[63]
A.J. Rubio-Montero,[57] R. Rui,[64] I. Rusanov,[66] G. Russo,[85] E. Ryabinkin,[16] A. Rybicki,[41] S. Sadovsky,[59]
K. Šafařík,[8] R. Sahoo,[53] J. Saini,[11] P. Saiz,[8] D. Sakata,[75] C.A. Salgado,[28] R. Salgueiro Domingues da Silva,[8]
S. Salur,[104] T. Samanta,[11] S. Sambyal,[51] V. Samsonov,[50] L. Šándor,[38] A. Sandoval,[10] M. Sano,[75] S. Sano,[14]
R. Santo,[43] R. Santoro,[20] J. Sarkamo,[32] P. Saturnini,[37] E. Scapparone,[26] F. Scarlassara,[53] R.P. Scharenberg,[113]
C. Schiaua,[22] R. Schicker,[66] H. Schindler,[8] C. Schmidt,[21] H.R. Schmidt,[21] K. Schossmaier,[8] S. Schreiner,[8]
S. Schuchmann,[25] J. Schukraft,[8] Y. Schutz,[27] K. Schwarz,[21] K. Schweda,[66] G. Scioli,[18] E. Scomparin,[17] P.A. Scott,[40]
G. Segato,[53] D. Semenov,[30] S. Senyukov,[78] J. Seo,[13] S. Serci,[87] L. Serkin,[80] E. Serradilla,[57] A. Sevcenco,[82]
I. Sgura,[20] G. Shabratova,[44] R. Shahoyan,[8] G. Sharkov,[15] N. Sharma,[7] S. Sharma,[51] K. Shigaki,[76]
M. Shimomura,[75] K. Shtejer,[4] Y. Sibiriak,[16] M. Siciliano,[35] E. Sicking,[8,dd] E. Siddi,[46] T. Siemiarczuk,[88]
A. Silenzi,[18] D. Silvermyr,[31] E. Simili,[73] G. Simonetti,[20,i] R. Singaraju,[11] R. Singh,[51] V. Singhal,[11] B.C. Sinha,[11]
T. Sinha,[63] B. Sitar,[92] M. Sitta,[78] T.B. Skaali,[1] K. Skjerdal,[19] R. Smakal,[54] N. Smirnov,[29] R. Snellings,[55]
H. Snow,[40] C. Søgaard,[45] A. Soloviev,[59] H.K. Soltveit,[66] R. Soltz,[96] W. Sommer,[25] C.W. Son,[72] H. Son,[101]
M. Song,[60] C. Soos,[8] F. Soramel,[53] D. Soyk,[21] M. Spyropoulou-Stassinaki,[49] B.K. Srivastava,[113] J. Stachel,[66]
F. Staley,[36] E. Stan,[82] G. Stefanek,[88] G. Stefanini,[8] T. Steinbeck,[2,b] E. Stenlund,[74] G. Steyn,[67] D. Stocco,[35,v]
R. Stock,[25] P. Stolpovsky,[59] P. Strmen,[92] A.A.P. Suaide,[84] M.A. Subieta Vásquez,[35] T. Sugitate,[76] C. Suire,[56]
M. Šumbera,[6] T. Susa,[24] D. Swoboda,[8] J. Symons,[104] A. Szanto de Toledo,[84] I. Szarka,[92] A. Szostak,[46]
M. Szuba,[106] M. Tadel,[8] C. Tagridis,[49] A. Takahara,[14] J. Takahashi,[71] R. Tanabe,[75] J.D. Tapia Takaki,[56]
H. Taureg,[8] A. Tauro,[8] M. Tavlet,[8] G. Tejeda Muñoz,[79] A. Telesca,[8] C. Terrevoli,[20] J. Thäder,[2,b] R. Tieulent,[70]
D. Tlusty,[54] A. Toia,[8] T. Tolyhy,[9] C. Torcato de Matos,[8] H. Torii,[76] G. Torralba,[2] L. Toscano,[17] F. Tosello,[17]
A. Tournaire,[27,ee] T. Traczyk,[106] P. Tribedy,[11] G. Tröger,[2] D. Truesdale,[23] W.H. Trzaska,[32] G. Tsiledakis,[66]
E. Tsilis,[49] T. Tsuji,[14] A. Tumkin,[42] R. Turrisi,[81] A. Turvey,[3] T.S. Tveter,[1] H. Tydesjö,[8] K. Tywoniuk,[1] J. Ulery,[25]
K. Ullaland,[19] A. Uras,[87] J. Urbán,[61] G.M. Urciuoli,[89] G.L. Usai,[87] A. Vacchi,[93] M. Vala,[44,ff] L. Valencia Palomo,[10]
S. Vallero,[66] N. van der Kolk,[55] P. Vande Vyvre,[8] M. van Leeuwen,[73] L. Vannucci,[112] A. Vargas,[79] R. Varma,[105]
A. Vasiliev,[16] I. Vassiliev,[2,cc] M. Vasileiou,[49] V. Vechernin,[30] M. Venaruzzo,[64] E. Vercellin,[35] S. Vergara,[79]
R. Vernet,[39,gg] M. Verweij,[73] I. Vetlitskiy,[15] L. Vickovic,[98] G. Viesti,[53] O. Vikhlyantsev,[42] Z. Vilakazi,[67]
O. Villalobos Baillie,[40] A. Vinogradov,[16] L. Vinogradov,[30] Y. Vinogradov,[42] T. Virgili,[85] Y.P. Viyogi,[11]
A. Vodopianov,[44] K. Voloshin,[15] S. Voloshin,[48] G. Volpe,[20] B. von Haller,[8] D. Vranic,[21] J. Vrláková,[61]
B. Vulpescu,[37] B. Wagner,[19] V. Wagner,[54] L. Wallet,[8] R. Wan,[68,l] D. Wang,[68] Y. Wang,[66] K. Watanabe,[75]
Q. Wen,[103] J. Wessels,[43] U. Westerhoff,[43] J. Wiechula,[66] J. Wikne,[1] A. Wilk,[43] G. Wilk,[88] M.C.S. Williams,[26]
N. Willis,[56] B. Windelband,[66] C. Xu,[68] C. Yang,[68] H. Yang,[66] S. Yasnopolskiy,[16] F. Yermia,[27] J. Yi,[72] Z. Yin,[68]
H. Yokoyama,[75] I-K. Yoo,[72] X. Yuan,[68,hh] V. Yurevich,[44] I. Yushmanov,[16] E. Zabrodin,[1] B. Zagreev,[15] A. Zalite,[50]
C. Zampolli,[8,ii] Yu. Zanevsky,[44] S. Zaporozhets,[44] A. Zarochentsev,[30] P. Závada,[109] H. Zbroszczyk,[106] P. Zelnicek,[2]
A. Zenin,[59] A. Zepeda,[69] I. Zgura,[82] M. Zhalov,[50] X. Zhang,[68,a] D. Zhou,[68] S. Zhou,[103] J. Zhu,[68]
A. Zichichi,[18,t] A. Zinchenko,[44] G. Zinovjev,[62] Y. Zoccarato,[70] V. Zycháček,[54] and M. Zynovyev[62]

[1]*Department of Physics, University of Oslo, Oslo, Norway*
[2]*Kirchhoff-Institut für Physik, Ruprecht-Karls-Universität Heidelberg, Heidelberg, Germany*
[3]*Physics Department, Creighton University, Omaha, NE, United States*
[4]*Centro de Aplicaciones Tecnológicas y Desarrollo Nuclear (CEADEN), Havana, Cuba*
[5]*Yerevan Physics Institute, Yerevan, Armenia*
[6]*Nuclear Physics Institute, Academy of Sciences of the Czech Republic, Řež u Prahy, Czech Republic*
[7]*Physics Department, Panjab University, Chandigarh, India*
[8]*European Organization for Nuclear Research (CERN), Geneva, Switzerland*

[9]*KFKI Research Institute for Particle and Nuclear Physics,*
Hungarian Academy of Sciences, Budapest, Hungary
[10]*Instituto de Física, Universidad Nacional Autónoma de México, Mexico City, Mexico*
[11]*Variable Energy Cyclotron Centre, Kolkata, India*
[12]*Department of Physics Aligarh Muslim University, Aligarh, India*
[13]*Gangneung-Wonju National University, Gangneung, South Korea*
[14]*University of Tokyo, Tokyo, Japan*
[15]*Institute for Theoretical and Experimental Physics, Moscow, Russia*
[16]*Russian Research Centre Kurchatov Institute, Moscow, Russia*
[17]*Sezione INFN, Turin, Italy*
[18]*Dipartimento di Fisica dell'Università and Sezione INFN, Bologna, Italy*
[19]*Department of Physics and Technology, University of Bergen, Bergen, Norway*
[20]*Dipartimento Interateneo di Fisica 'M. Merlin' and Sezione INFN, Bari, Italy*
[21]*Research Division and ExtreMe Matter Institute EMMI,*
GSI Helmholtzzentrum für Schwerionenforschung, Darmstadt, Germany
[22]*National Institute for Physics and Nuclear Engineering, Bucharest, Romania*
[23]*Department of Physics, Ohio State University, Columbus, OH, United States*
[24]*Rudjer Bošković Institute, Zagreb, Croatia*
[25]*Institut für Kernphysik, Johann Wolfgang Goethe-Universität Frankfurt, Frankfurt, Germany*
[26]*Sezione INFN, Bologna, Italy*
[27]*SUBATECH, Ecole des Mines de Nantes, Université de Nantes, CNRS-IN2P3, Nantes, France*
[28]*Departamento de Física de Partículas and IGFAE,*
Universidad de Santiago de Compostela, Santiago de Compostela, Spain
[29]*Yale University, New Haven, CT, United States*
[30]*V. Fock Institute for Physics, St. Petersburg State University, St. Petersburg, Russia*
[31]*Oak Ridge National Laboratory, Oak Ridge, TN, United States*
[32]*Helsinki Institute of Physics (HIP) and University of Jyväskylä, Jyväskylä, Finland*
[33]*Frankfurt Institute for Advanced Studies, Johann Wolfgang Goethe-Universität Frankfurt, Frankfurt, Germany*
[34]*Sezione INFN, Catania, Italy*
[35]*Dipartimento di Fisica Sperimentale dell'Università and Sezione INFN, Turin, Italy*
[36]*Commissariat à l'Energie Atomique, IRFU, Saclay, France*
[37]*Laboratoire de Physique Corpusculaire (LPC), Clermont Université,*
Université Blaise Pascal, CNRS–IN2P3, Clermont-Ferrand, France
[38]*Institute of Experimental Physics, Slovak Academy of Sciences, Košice, Slovakia*
[39]*Dipartimento di Fisica e Astronomia dell'Università and Sezione INFN, Catania, Italy*
[40]*School of Physics and Astronomy, University of Birmingham, Birmingham, United Kingdom*
[41]*The Henryk Niewodniczanski Institute of Nuclear Physics, Polish Academy of Sciences, Cracow, Poland*
[42]*Russian Federal Nuclear Center (VNIIEF), Sarov, Russia*
[43]*Institut für Kernphysik, Westfälische Wilhelms-Universität Münster, Münster, Germany*
[44]*Joint Institute for Nuclear Research (JINR), Dubna, Russia*
[45]*Niels Bohr Institute, University of Copenhagen, Copenhagen, Denmark*
[46]*Sezione INFN, Cagliari, Italy*
[47]*Institut Pluridisciplinaire Hubert Curien (IPHC),*
Université de Strasbourg, CNRS-IN2P3, Strasbourg, France
[48]*Wayne State University, Detroit, MI, United States*
[49]*Physics Department, University of Athens, Athens, Greece*
[50]*Petersburg Nuclear Physics Institute, Gatchina, Russia*
[51]*Physics Department, University of Jammu, Jammu, India*
[52]*Laboratori Nazionali di Frascati, INFN, Frascati, Italy*
[53]*Dipartimento di Fisica dell'Università and Sezione INFN, Padova, Italy*
[54]*Faculty of Nuclear Sciences and Physical Engineering,*
Czech Technical University in Prague, Prague, Czech Republic
[55]*Nikhef, National Institute for Subatomic Physics, Amsterdam, Netherlands*
[56]*Institut de Physique Nucléaire d'Orsay (IPNO),*
Université Paris-Sud, CNRS-IN2P3, Orsay, France
[57]*Centro de Investigaciones Energéticas Medioambientales y Tecnológicas (CIEMAT), Madrid, Spain*
[58]*Moscow Engineering Physics Institute, Moscow, Russia*
[59]*Institute for High Energy Physics, Protvino, Russia*
[60]*Yonsei University, Seoul, South Korea*
[61]*Faculty of Science, P.J. Šafárik University, Košice, Slovakia*
[62]*Bogolyubov Institute for Theoretical Physics, Kiev, Ukraine*
[63]*Saha Institute of Nuclear Physics, Kolkata, India*
[64]*Dipartimento di Fisica dell'Università and Sezione INFN, Trieste, Italy*
[65]*Institut für Kernphysik, Technische Universität Darmstadt, Darmstadt, Germany*

[66]*Physikalisches Institut, Ruprecht-Karls-Universität Heidelberg, Heidelberg, Germany*
[67]*Physics Department, University of Cape Town,*
iThemba Laboratories, Cape Town, South Africa
[68]*Hua-Zhong Normal University, Wuhan, China*
[69]*Centro de Investigación y de Estudios Avanzados (CINVESTAV), Mexico City and Mérida, Mexico*
[70]*Université de Lyon, Université Lyon 1, CNRS/IN2P3, IPN-Lyon, Villeurbanne, France*
[71]*Universidade Estadual de Campinas (UNICAMP), Campinas, Brazil*
[72]*Pusan National University, Pusan, South Korea*
[73]*Nikhef, National Institute for Subatomic Physics and Institute*
for Subatomic Physics of Utrecht University, Utrecht, Netherlands
[74]*Division of Experimental High Energy Physics, University of Lund, Lund, Sweden*
[75]*University of Tsukuba, Tsukuba, Japan*
[76]*Hiroshima University, Hiroshima, Japan*
[77]*Zentrum für Technologietransfer und Telekommunikation (ZTT), Fachhochschule Worms, Worms, Germany*
[78]*Dipartimento di Scienze e Tecnologie Avanzate dell'Università del*
Piemonte Orientale and Gruppo Collegato INFN, Alessandria, Italy
[79]*Benemérita Universidad Autónoma de Puebla, Puebla, Mexico*
[80]*Instituto de Ciencias Nucleares, Universidad Nacional Autónoma de México, Mexico City, Mexico*
[81]*Sezione INFN, Padova, Italy*
[82]*Institute of Space Sciences (ISS), Bucharest, Romania*
[83]*Institute of Physics, Bhubaneswar, India*
[84]*Universidade de São Paulo (USP), São Paulo, Brazil*
[85]*Dipartimento di Fisica 'E.R. Caianiello' dell'Università and Sezione INFN, Salerno, Italy*
[86]*Sezione INFN, Bari, Italy*
[87]*Dipartimento di Fisica dell'Università and Sezione INFN, Cagliari, Italy*
[88]*Soltan Institute for Nuclear Studies, Warsaw, Poland*
[89]*Sezione INFN, Rome, Italy*
[90]*University of Houston, Houston, TX, United States*
[91]*Laboratoire de Physique Subatomique et de Cosmologie (LPSC), Université Joseph Fourier,*
CNRS-IN2P3, Institut Polytechnique de Grenoble, Grenoble, France
[92]*Faculty of Mathematics, Physics and Informatics, Comenius University, Bratislava, Slovakia*
[93]*Sezione INFN, Trieste, Italy*
[94]*Budker Institute for Nuclear Physics, Novosibirsk, Russia*
[95]*Sección Física, Departamento de Ciencias, Pontificia Universidad Católica del Perú, Lima, Peru*
[96]*Lawrence Livermore National Laboratory, Livermore, CA, United States*
[97]*Universidad Autónoma de Sinaloa, Culiacán, Mexico*
[98]*Technical University of Split FESB, Split, Croatia*
[99]*Institute for Nuclear Research, Academy of Sciences, Moscow, Russia*
[100]*University of Tennessee, Knoxville, TN, United States*
[101]*Department of Physics, Sejong University, Seoul, South Korea*
[102]*Faculty of Engineering, Bergen University College, Bergen, Norway*
[103]*China Institute of Atomic Energy, Beijing, China*
[104]*Lawrence Berkeley National Laboratory, Berkeley, CA, United States*
[105]*Indian Institute of Technology, Mumbai, India*
[106]*Warsaw University of Technology, Warsaw, Poland*
[107]*California Polytechnic State University, San Luis Obispo, CA, United States*
[108]*Fachhochschule Köln, Köln, Germany*
[109]*Institute of Physics, Academy of Sciences of the Czech Republic, Prague, Czech Republic*
[110]*Dipartimento di Fisica dell'Università 'La Sapienza' and Sezione INFN, Rome, Italy*
[111]*Physics Department, University of Rajasthan, Jaipur, India*
[112]*Laboratori Nazionali di Legnaro, INFN, Legnaro, Italy*
[113]*Purdue University, West Lafayette, IN, United States*

(Dated: June 29, 2010)

The ratio of the yields of antiprotons to protons in pp collisions has been measured by the ALICE experiment at $\sqrt{s} = 0.9$ and 7 TeV during the initial running periods of the Large Hadron Collider(LHC). The measurement covers the transverse momentum interval $0.45 < p_{\mathrm{t}} < 1.05$ GeV/c and rapidity $|y| < 0.5$. The ratio is measured to be $R_{|y|<0.5} = 0.957 \pm 0.006(stat.) \pm 0.014(syst.)$ at 0.9 TeV and $R_{|y|<0.5} = 0.991 \pm 0.005(stat.) \pm 0.014(syst.)$ at 7 TeV and it is independent of both rapidity and transverse momentum. The results are consistent with the conventional model of baryon-number transport and set stringent limits on any additional contributions to baryon-number transfer over very large rapidity intervals in pp collisions.

In inelastic non-diffractive proton-proton collisions at very high energy, the incoming projectile breaks up into several hadrons which emerge after the collision in general under small angles along the original beam direction. The deceleration of the incoming proton, or more precisely of the conserved baryon number associated with the beam particles, is often called "baryon-number transport" and has been debated theoretically for some time [1–7].

One mechanism responsible for baryon-number transport is the break-up of the proton into a diquark–quark configuration [2]. The diquark hadronizes after the reaction with some longitudinal momentum p_z into a new particle, which carries the baryon number of the incoming proton. This baryon-number transport is usually quantified in terms of the rapidity loss $\Delta y = y_{\rm beam} - y_{\rm baryon}$, where $y_{\rm beam}$ ($y_{\rm baryon}$) is the rapidity of the incoming beam (outgoing baryon)[1].

However, diquarks in general retain a large fraction of the proton momentum and therefore stay close to beam rapidity, typically within one or two units. Therefore, additional processes have been proposed to transport the baryon number over larger distances in rapidity, in particular via purely gluonic exchanges, where the proton breaks up into three quarks. The baryon number resides with a non-perturbative configuration of gluon fields, the so-called "baryon string junction", which connects the valence quarks [1, 3]. In this picture, baryon-number transport is suppressed exponentially with the rapidity interval Δy, proportional to $\exp\left[(\alpha_{\rm J} - 1)\,\Delta y\right]$, where $\alpha_{\rm J}$ is identified in the Regge model as the intercept of the trajectory for the corresponding exchange in the t-channel. If the string junction intercept is approximated with the one of the standard Reggeon (or meson), $\alpha_{\rm J} \approx 0.5$, baryon transport will approach zero with increasing Δy. If the intercept of the pure string junction is $\alpha_{\rm J} \approx 1$, as motivated by perturbative QCD [4], it will approach a constant and finite value.

The LHC, being by far the highest energy proton–proton collider, opens the possibility to investigate baryon transport over very large rapidity intervals by measuring the antiproton-to-proton production ratio at midrapidity, $R = N_{\overline{\rm p}}/N_{\rm p}$, or equivalently, the proton–antiproton asymmetry, $A = (N_{\rm p} - N_{\overline{\rm p}})/(N_{\rm p} + N_{\overline{\rm p}})$. Most

---

[a] Also at Laboratoire de Physique Corpusculaire (LPC), Clermont Université, Université Blaise Pascal, CNRS–IN2P3, Clermont-Ferrand, France

[b] Also at Frankfurt Institute for Advanced Studies, Johann Wolfgang Goethe-Universität Frankfurt, Frankfurt, Germany

[c] Now at Sezione INFN, Padova, Italy

[d] Now at Research Division and ExtreMe Matter Institute EMMI, GSI Helmholtzzentrum für Schwerionenforschung, Darmstadt, Germany

[e] Now at Institut für Kernphysik, Johann Wolfgang Goethe-Universität Frankfurt, Frankfurt, Germany

[f] Now at Physics Department, University of Cape Town, iThemba Laboratories, Cape Town, South Africa

[g] Now at National Institute for Physics and Nuclear Engineering, Bucharest, Romania

[h] Also at University of Houston, Houston, TX, United States

[i] Now at European Organization for Nuclear Research (CERN), Geneva, Switzerland

[j] Also at Dipartimento di Fisica dell´Università, Udine, Italy

[k] Now at Helsinki Institute of Physics (HIP) and University of Jyväskylä, Jyväskylä, Finland

[l] Now at Institut Pluridisciplinaire Hubert Curien (IPHC), Université de Strasbourg, CNRS-IN2P3, Strasbourg, France

[m] Now at Institut für Kernphysik, Westfälische Wilhelms-Universität Münster, Münster, Germany

[n] Now at : University of Technology and Austrian Academy of Sciences, Vienna, Austria

[o] Also at Lawrence Livermore National Laboratory, Livermore, CA, United States

[p] Also at European Organization for Nuclear Research (CERN), Geneva, Switzerland

[q] Deceased

[r] Now at Yale University, New Haven, CT, United States

[s] Now at University of Tsukuba, Tsukuba, Japan

[t] Also at Centro Fermi – Centro Studi e Ricerche e Museo Storico della Fisica "Enrico Fermi", Rome, Italy

[u] Also at Laboratoire de Physique Subatomique et de Cosmologie (LPSC), Université Joseph Fourier, CNRS-IN2P3, Institut Polytechnique de Grenoble, Grenoble, France

[v] Now at SUBATECH, Ecole des Mines de Nantes, Université de Nantes, CNRS-IN2P3, Nantes, France

[w] Now at Dipartimento di Fisica Sperimentale dell'Università and Sezione INFN, Turin, Italy

[x] Now at Commissariat à l'Energie Atomique, IRFU, Saclay, France

[y] Also at Department of Physics, University of Oslo, Oslo, Norway

[z] Also at Wrocław University, Wrocław, Poland

[aa] Now at Physikalisches Institut, Ruprecht-Karls-Universität Heidelberg, Heidelberg, Germany

[bb] Now at Department of Physics and Technology, University of Bergen, Bergen, Norway

[cc] Now at Physics Department, University of Athens, Athens, Greece

[dd] Also at Institut für Kernphysik, Westfälische Wilhelms-Universität Münster, Münster, Germany

[ee] Now at Université de Lyon, Université Lyon 1, CNRS/IN2P3, IPN-Lyon, Villeurbanne, France

[ff] Now at Faculty of Science, P.J. Šafárik University, Košice, Slovakia

[gg] Now at : Centre de Calcul IN2P3, Lyon, France

[hh] Also at Dipartimento di Fisica dell'Università and Sezione INFN, Padova, Italy

[ii] Also at Sezione INFN, Bologna, Italy

[1] The rapidity y is defined as $y = 0.5\ln\left[(E + p_z)\,/\,(E - p_z)\right]$; rapidity $y = 0$ corresponds to longitudinal momentum $p_z = 0$ of the baryon in the center-of-mass system and $\Delta y = \ln\left(\sqrt{s}/m_{\rm p}\right)$.

of the (anti)protons at midrapidity are created in baryon–antibaryon pair production, implying equal yields. Any excess of protons over antiprotons is therefore associated with the baryon-number transfer from the incoming beam. Note that such a study has not been carried out in high-energy proton–antiproton colliders (Sp$\overline{\text{p}}$S, Tevatron) because of the symmetry of the initial system at midrapidity. Model predictions for the ratio R at LHC energies range from unity, i.e., no baryon-number transfer to midrapidity, down to about 0.9 in models where the string junction transfer is not suppressed with the rapidity interval ($\alpha_{\rm J} \approx 1$).

In this letter, we describe the measurement of the $\overline{\text{p}}$/p ratio at midrapidity in non-diffractive pp collisions at center-of-mass energies $\sqrt{s}$ = 0.9 TeV and 7 TeV ($\Delta y \approx 6.9$–8.9), with the ALICE experiment at the LHC.

ALICE, which is the dedicated heavy-ion detector at the LHC, consists of 18 detector sub-systems [8, 9]. The central tracking systems used in the present analysis are located inside a solenoidal magnet (B = 0.5 T); they are optimized to provide good momentum resolution and particle identification (PID) over a broad momentum range, up to the highest multiplicities expected for heavy ion collisions at the LHC. All detector systems were commissioned and aligned during several months of cosmic-ray data-taking in 2008 and 2009 [10, 11].

Collisions occur inside a beryllium vacuum pipe (3 cm in radius and 800 μm thick) at the center of the ALICE detector. The tracking system in the ALICE central barrel has full azimuth coverage within the pseudo-rapidity window $|\eta| < 0.9$. The following detector sub-systems were used in this analysis: the *Inner Tracking System* (ITS) [11], the *Time Projection Chamber* (TPC) [12] and the VZERO detector [8].

The ITS consists of six cylindrical layers of silicon detectors with radii of 3.9/7.6 cm (Silicon Pixel Detectors–SPD), 15.0/23.9 cm (Silicon Drift Detectors–SDD) and 38/43 cm (Silicon Strip Detectors–SSD). They provide full azimuth coverage for tracks matching the acceptance of the TPC ($|\eta| < 0.9$).

The TPC is the main tracking detector of the central barrel. The detector is cylindrical in shape with an active volume of inner radius 85 cm, outer radius of 250 cm and an overall length along the beam direction of 500 cm.

Finally, the VZERO detector consists of two arrays of 32 scintillators each, which are placed around the beam pipe on either side of the interaction region) at $z = 3.3$ m and $z = -0.9$ m, covering the pseudorapidity ranges $2.8 < \eta < 5.1$ and $-3.7 < \eta < -1.7$, respectively [13]. A detailed description of the ALICE detectors, its components, and their performance can be found in [8].

Data from 2.8 ($\sqrt{s} = 0.9$ TeV) and 4.2 ($\sqrt{s} = 7$ TeV) million pp collisions, recorded during the first LHC runs (December 2009, March–April 2010) were used for this analysis. The events were recorded with both field polarities for each energy. The trigger required a hit in one of the VZERO counters or in the SPD detector, i.e., at least one charged particle anywhere in the 8 units of pseudorapidity covered by these trigger detectors [13]. In addition, the trigger required a coincidence between the signals from two beam pick-up counters, one on each side of the interaction region, indicating the presence of passing bunches.

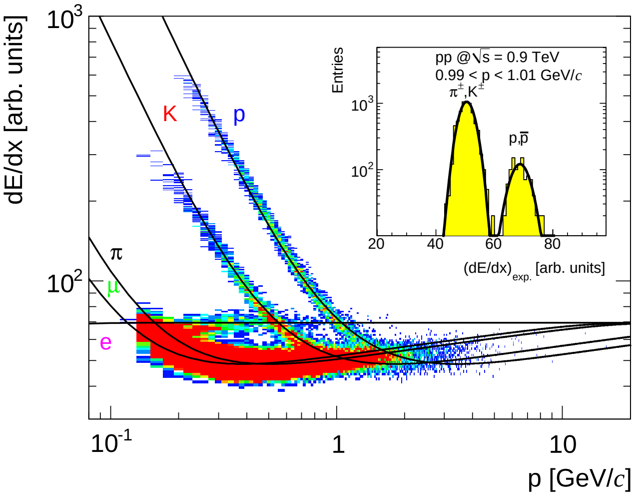

FIG. 1. (Color online) The measured ionization per unit length as a function of particle momentum (both charges) in the TPC gas. The curves correspond to expected energy loss [14] for different particle types. The inset shows the measured ionization for tracks with $0.99 < p < 1.01$ GeV/c. The lines are Gaussian fits to the data.

Beam-induced background was reduced to a negligible level (< 0.01%) with the help of the timing information from the VZERO counters [13] and by requiring a reconstructed primary vertex (calculated from the SPD) within ±1 cm perpendicular to and ±10 cm along the beam axis.

Measurements of momentum and particle identification are performed using information from the TPC detector, which measures the ionization in the TPC gas and the particle trajectory with up to 159 space points. In order to ensure a good track quality, a minimum of 80 clusters was required per track in the TPC and at least two hits in the ITS of which at least one is in the SPD. In order to reduce the contamination from background and secondary tracks (e.g. (anti)protons originating from weak hyperon decays or secondary interactions in the material), a cut was imposed on the distance of closest approach (*dca*) of the track to the primary vertex in the *xy* (transverse) plane, which varied from 2.65 to 1.8 mm (2.33 to 1.5 mm for the 7 TeV data) for the lowest ($0.45 < p_{\rm t} < 0.55$ GeV/c) and highest ($0.95 < p_{\rm t} < 1.05$ GeV/c) $p_{\rm t}$ bins, respectively. This cut corresponds to 5σ of the measured *dca* resolution for

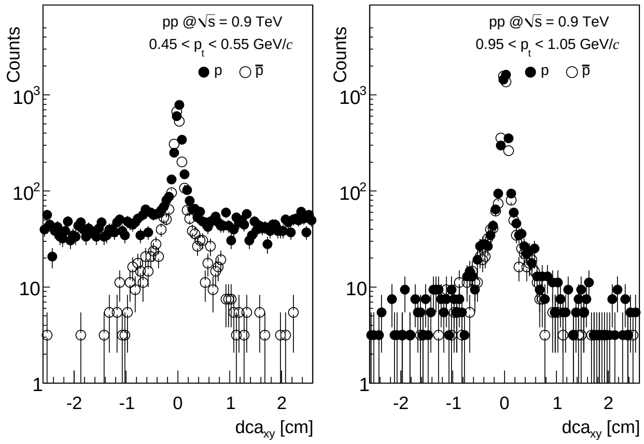

FIG. 2. The distance of closest approach (*dca*) distributions of p and $\overline{\mathrm{p}}$ for the lowest (left plot) and highest (right plot) transverse momentum bins. The broad background of protons at low momentum originates from secondary particles created in the detector material, whereas the tails for both p and $\overline{\mathrm{p}}$ at high momentum (and for $\overline{\mathrm{p}}$ at low momentum) arise from weak hyperon decays.

each momentum bin.

Particles are identified using their specific ionization ($\mathrm{d}E/\mathrm{d}x$) in the TPC gas [12]. Figure 1 shows the ionization (truncated mean) as a function of particle momentum together with the expected curves [14] for different particle species. The inset shows the measured $\mathrm{d}E/\mathrm{d}x$ for tracks in the momentum range $0.99 < p < 1.01$ GeV/c with clearly separated peaks for (anti)protons and lighter particles. The $\mathrm{d}E/\mathrm{d}x$ resolution of the TPC is 5, depending slightly on the number of TPC clusters and the track inclination angle. For this analysis, (anti)protons were selected within a band of $\pm 3\sigma$ around the expected value.

In order to assure uniform geometrical acceptance, high reconstruction efficiency and unambiguous proton identification, we restrict the analysis to protons and antiprotons in the rapidity range $|y| < 0.5$ and the momentum range $0.45 < p < 1.05$ GeV/c. The contamination of the proton sample with electrons or pions and kaons is negligible ($< 0.1\%$) even at the highest momentum bins, and in addition essentially charge symmetric.

Most instrumental effects associated with the acceptance, reconstruction efficiency, and resolution are identical for primary protons and anti-protons and therefore cancel in the ratio. However, because of significant differences in the relevant cross sections, anti-protons are more likely than protons to be absorbed or elastically scattered[2] within the detector, and a non negligible background in the proton sample arises from secondary interactions in the beam pipe and inner layers of the detector.

In order to correct for the difference between p–A and $\overline{\mathrm{p}}$–A elastic and inelastic reactions in the detector material, detailed Monte Carlo simulations based on GEANT3 [15] and FLUKA [16] were performed. These corrections rely in particular on the proper description of the interaction cross sections used as input by the transport models. These values were therefore compared with experimental measurements [17, 18]. While p–A cross sections are similar in both models and in agreement with existing data, GEANT3 (as well as the current version of GEANT4) significantly overestimates the measured inelastic cross sections for antiprotons in the relevant momentum range by about a factor of two, whereas FLUKA describes the data very well. Concerning elastic scattering, where only a limited data set is available for comparison, GEANT3 cross sections are about 25% above FLUKA, the latter being again closer to the measurements. We therefore used the FLUKA results to account for the difference of p and $\overline{\mathrm{p}}$ cross sections, which amount to a correction of the $\overline{\mathrm{p}}$/p ratio by 8% and 3.5% for absorption and elastic scattering, respectively.

The contamination of the proton sample due to secondaries originating from interactions with the detector material was directly measured with the data and subtracted. Most of these background tracks do not point back to the interaction vertex and can therefore be excluded with a *dca* cut. Figure 2 shows the *dca* distributions of p and $\overline{\mathrm{p}}$ for the lowest (left panel) and the highest (right panel) transverse momentum bins. Secondary protons are clearly visible in the left plot due to their wide *dca* distribution. At higher momenta the background of secondary protons becomes very small. The remaining tails visible in the *dca* distributions are due to (anti)protons originating from weak decays. The background of secondary protons, which remains after the *dca* cut under the peak of primaries, is subtracted by determining its shape from Monte Carlo simulations and adjusting the amount to the data at large values of the *dca*. This correction is calculated and applied differentially as a function of y and p_{t}; it varies between 14% for the lowest and less than 0.3% for the highest transverse momentum bins.

The contamination coming from feed-down (i.e., (anti)protons originating from the weak decay of Λ and $\overline{\Lambda}$) was subtracted in a similar way by parametrization and fitting to the data of the respective simulated *dca* distributions. This correction ranges from 20% to 12% for the lowest and highest p_{t} bins, respectively.

---

[2] Particles undergoing elastic scattering in the inner detectors can still be reconstructed in the TPC but the corresponding ITS hits will in general not be associated to the track if the scattering angle is large.

TABLE I. Systematic uncertainties of the $\overline{\mathrm{p}}/\mathrm{p}$ ratio.

Systematic Uncertainty	
Material budget	0.5%
Absorption cross section	0.8%
Elastic cross section	0.8%
Analysis cuts	0.4%
Corrections (secondaries/feed-down)	0.6%
Total	1.4%

The main sources of systematic uncertainties are the detector material budget, the (anti)proton reaction cross section, the subtraction of secondary protons and the accuracy of the detector response simulations (see Table I). The amount of material in the central part of ALICE is very low, corresponding to about 10% of a radiation length on average between the vertex and the active volume of the TPC. It has been studied with collision data and adjusted in the simulation based on the analysis of photon conversions. The current simulation reproduces the amount and spatial distribution of reconstructed conversion points in great detail, with a relative accuracy of a few percent. Based on these studies, we assign a systematic uncertainty of 7% to the material budget. By changing the material in the simulation by this amount, we find a variation of the final ratio R of less than 0.5%.

The experimentally measured $\overline{\mathrm{p}}$–A reaction cross sections are determined with a typical accuracy better than 5% [17]. We assign a 10% uncertainty to the absorption correction as calculated with FLUKA, which leads to a 0.8% uncertainty in the ratio R. By comparing GEANT3 with FLUKA and with the experimentally measured elastic cross-sections, the corresponding uncertainty was estimated to be 0.8%, which corresponds to the difference between the correction factors calculated with the two models.

By changing the event selection, analysis cuts and track quality requirements within reasonable ranges, we find a maximum deviation of the results of 0.4%, which we assign as systematic uncertainty to the accuracy of the detector simulation and analysis corrections.

The uncertainty resulting from the subtraction of secondary protons and from the feed-down corrections was estimated to be 0.6% by using different functional forms for the background subtraction and for the contribution of the hyperon decay products.

The contribution of diffractive reactions to our final event sample was studied with different event generators and was found to be less than 3%, resulting into a negligible contribution ($< 0.1\%$) to the systematic uncertainty.

Finally, the complete analysis was repeated using only TPC information (i.e., without using any of the ITS detectors). The resulting difference was negligible at both energies ($< 0.1\%$).

Table I summarizes the contribution to the systematic uncertainty from all the different sources. The total systematic uncertainty is identical for both energies and amounts to 1.4%.

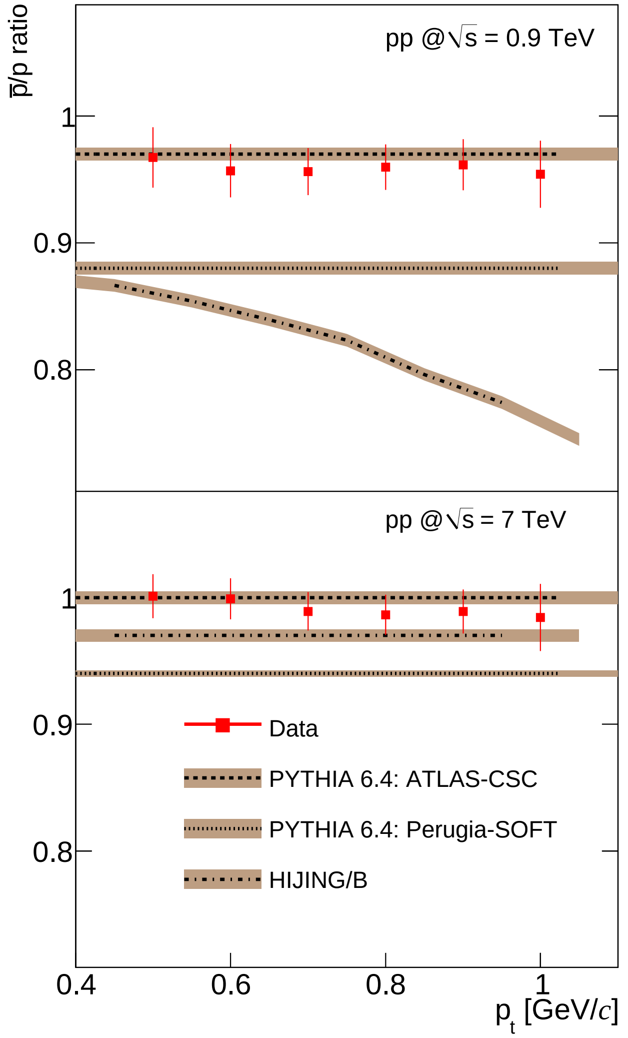

FIG. 3. (Color online) The p_{t} dependence of the $\overline{\mathrm{p}}/\mathrm{p}$ ratio integrated over $|y| < 0.5$ for pp collisions at $\sqrt{s} = 0.9$ TeV (top) and $\sqrt{s} = 7$ TeV (bottom). Only statistical errors are shown for the data; the width of the Monte Carlo bands indicates the statistical uncertainty of the simulation results.

The final, feed-down corrected $\overline{\mathrm{p}}/\mathrm{p}$ ratio R integrated within our rapidity and p_{t} acceptance rises from $R_{|y|<0.5} = 0.957 \pm 0.006(stat.) \pm 0.014(syst.)$ at $\sqrt{s} = 0.9$ TeV to $R_{|y|<0.5} = 0.991 \pm 0.005(stat.) \pm 0.014(syst.)$ at $\sqrt{s} = 7$ TeV. The difference in the $\overline{\mathrm{p}}/\mathrm{p}$ ratio, $0.034 \pm 0.008(stat.)$, is significant because the systematic errors at both energies are fully correlated.

Within statistical errors, the measured ratio R shows no dependence on transverse momentum (Fig. 3) or rapidity (data not shown). The ratio is also independent of momentum and rapidity for all generators in our acceptance, with the exception of HIJING/B, which predicts

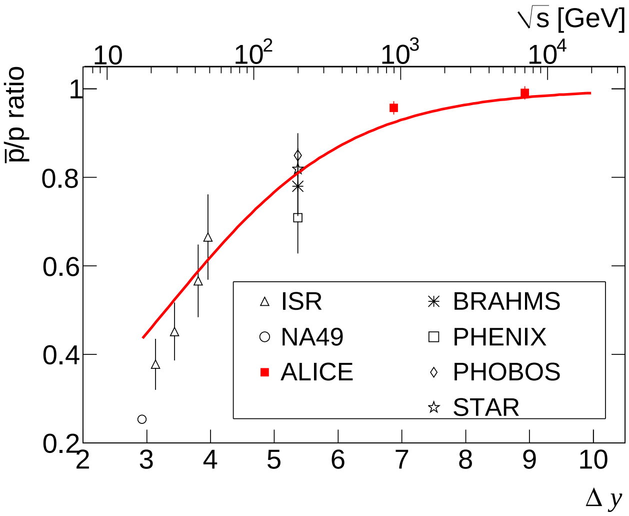

FIG. 4. (Color online) Central rapidity $\overline{\mathrm{p}}/\mathrm{p}$ ratio as a function of the rapidity interval Δy (lower axis) and center-of-mass energy (upper axis). Error bars correspond to the quadratic sum of statistical and systematic uncertainties for the RHIC and LHC measurements and to statistical errors otherwise.

a decrease with increasing transverse momentum for the lower energy.

The data are compared with various model predictions for pp collisions [6, 7, 19] in Table II (integrated values) and Fig. 3. The analytical QGSM model does not predict the p_t dependence and is therefore not included in Fig. 3. For both energies, two of the PYTHIA tunes [19] (ATLAS-CSC and Perugia-0) as well as the version of Quark–Gluon String Model (QGSM) with the value of the string junction intercept $\alpha_\mathrm{J} = 0.5$ [6] describe the experimental values well, whereas QGSM without string junctions ($\epsilon = 0$, ϵ is a parameter proportional to the probability of the string-junction exchange) is slightly above the data. HIJING/B [7], unlike the above models, includes a particular implementation of gluonic string junctions to enhance baryon-number transfer. This model underestimates the experimental results, in particular at the lower LHC energy. Also, QGSM with a value of the junction intercept $\alpha_\mathrm{J} = 0.9$ [6] predicts a smaller ratio, as does the Perugia-SOFT tune of PYTHIA, which also includes enhanced baryon transfer[3].

Figure 4 shows a compilation of central rapidity measurements of the ratio R in pp collisions as a function of center-of-mass energy (upper axis) and the rapidity interval Δy (lower axis). The ALICE measurements correspond to $\Delta y = 6.87$ and $\Delta y = 8.92$ for the two energies, whereas the lower energy data points are taken from [20–22]. The $\overline{\mathrm{p}}/\mathrm{p}$ ratio rises from 0.25 and 0.3 at the SPS and the lowest ISR energy, respectively, to a value of about 0.8 at $\sqrt{s} = 200$ GeV, indicating that a substantial fraction of the baryon number associated with the beam particles is transported over rapidity intervals of up to five units.

Although our measured midrapidity ratio R at $\sqrt{s} = 0.9$ TeV is close to unity, there is still a small but significant excess of protons over antiprotons corresponding to a p–$\overline{\mathrm{p}}$ asymmetry of $A = 0.022 \pm 0.003(stat.) \pm 0.007(syst.)$. On the other hand, the ratio at $\sqrt{s} = 7$ TeV is consistent with unity ($A = 0.005 \pm 0.003(stat.) \pm 0.007(syst.)$), which sets a stringent limit on the amount of baryon transport over 9 units in rapidity. The existence of a large value for the asymmetry even at infinite energy, which has been predicted to be $A = 0.035$ using $\alpha_\mathrm{J} = 1$ [4], is therefore excluded.

A rough approximation of the Δy dependence of the ratio R can be derived in the Regge model, where baryon pair production at very high energy is governed by Pomeron exchange and baryon transport by string-junction exchange [5]. In this case the p/$\overline{\mathrm{p}}$ ratio takes the simple form $1/R = 1 + C\exp[(\alpha_\mathrm{J} - \alpha_\mathrm{P})\Delta y]$. We have fitted such a function to the data, using as value for the Pomeron intercept $\alpha_\mathrm{P} = 1.2$ [23] and $\alpha_\mathrm{J} = 0.5$, whereas C, which determines the relative contributions of the two diagrams, is adjusted to the measurements from ISR, RHIC, and LHC. The fit, shown in Fig. 4, gives a reasonable description of the data with only one free parameter (C), except at lower energies, where contributions of other diagrams cannot be neglected [5]. Adding a second string junction diagram with a larger intercept [4], i.e., $1/R = 1 + C\exp[(\alpha_\mathrm{J} - \alpha_\mathrm{P})\Delta y] + C'\exp[(\alpha_{\mathrm{J}'} - \alpha_\mathrm{P})\Delta y]$ with $\alpha_{\mathrm{J}'} = 1$, does not improve the quality of the fit and its contribution is compatible with zero ($C \approx 10$, $C' \approx -0.1 \pm 0.1$). In a similar spirit, our data could also be used to constrain other Regge-model inspired descriptions of baryon asymmetry, for example when the string-junction exchange is replaced by the "odderon", which is the analogue of the Pomeron with odd C-parity; see [6].

In summary, we have measured the ratio of antiproton to proton production in the ALICE experiment at the CERN LHC collider at $\sqrt{s} = 0.9$ and $\sqrt{s} = 7$ TeV. Within our acceptance region ($|y| < 0.5$, $0.45 < p_\mathrm{t} < 1.05$ GeV/c), the ratio of antiproton-to-proton yields rises from $R_{|y|<0.5} = 0.957 \pm 0.006(stat.) \pm 0.014(syst.)$ at 0.9 to a value close to unity $R_{|y|<0.5} = 0.991 \pm 0.005(stat.) \pm 0.014(syst.)$ at 7 TeV. The $\overline{\mathrm{p}}/\mathrm{p}$ ratio is independent of both rapidity and transverse momentum. These results are consistent with standard models of baryon-number transport and set tight limits on any additional contributions to baryon-number transfer over very large rapidity intervals in pp collisions.

---

[3] We have checked that baryon transfer is the main reason for the different $\overline{\mathrm{p}}/\mathrm{p}$ ratios predicted by the models; the absolute yield of (anti)protons in our acceptance, which is dominated by pair production, is reproduced by the models to within ±20%.

TABLE II. The measured central rapidity $\overline{\mathrm{p}}/\mathrm{p}$ ratio compared to the predictions of different models (the statistical uncertainty in the models is less than 0.005). The quoted errors for the ALICE points are the quadratic sum of statistical and systematic uncertainties.

	Energy [TeV]	0.9	7
ALICE		0.957 ± 0.015	0.991 ± 0.015
PYTHIA	ATLAS-CSC Tune (306)	0.96	1.0
	Perugia-0 Tune (320)	0.95	1.0
	Perugia-SOFT Tune (322)	0.88	0.94
QGSM	$\epsilon = 0$	0.98	1.0
	$\epsilon = 0.076$, $\alpha_{\mathrm{J}} = 0.5$	0.96	0.99
	$\epsilon = 0.024$, $\alpha_{\mathrm{J}} = 0.9$	0.89	0.95
HIJING/B		0.83	0.97

ACKNOWLEDGEMENTS

We would like to thank Paola Sala, Alfredo Ferrari, Dmitri Kharzeev, Carlos Merino, Torbjörn Sjöstrand and Peter Skands for numerous and fruitful discussions on different topics of this paper.

The ALICE collaboration would like to thank all its engineers and technicians for their invaluable contributions to the construction of the experiment and the CERN accelerator teams for the outstanding performance of the LHC complex.

The ALICE collaboration acknowledges the following funding agencies for their support in building and running the ALICE detector: Calouste Gulbenkian Foundation from Lisbon and Swiss Fonds Kidagan, Armenia; Conselho Nacional de Desenvolvimento Científico e Tecnológico (CNPq), Financiadora de Estudos e Projetos (FINEP), Fundação de Amparo à Pesquisa do Estado de São Paulo (FAPESP); National Natural Science Foundation of China (NSFC), the Chinese Ministry of Education (CMOE) and the Ministry of Science and Technology of China (MSTC); Ministry of Education and Youth of the Czech Republic; Danish Natural Science Research Council, the Carlsberg Foundation and the Danish National Research Foundation; The European Research Council under the European Community's Seventh Framework Programme; Helsinki Institute of Physics and the Academy of Finland; French CNRS-IN2P3, the 'Region Pays de Loire', 'Region Alsace', 'Region Auvergne' and CEA, France; German BMBF and the Helmholtz Association; Hungarian OTKA and National Office for Research and Technology (NKTH); Department of Atomic Energy and Department of Science and Technology of the Government of India; Istituto Nazionale di Fisica Nucleare (INFN) of Italy; MEXT Grant-in-Aid for Specially Promoted Research, Japan; Joint Institute for Nuclear Research, Dubna; Korea Foundation for International Cooperation of Science and Technology (KICOS); CONACYT, DGAPA, México, ALFA-EC and the HELEN Program (High-Energy physics Latin-American–European Network); Stichting voor Fundamenteel Onderzoek der Materie (FOM) and the Nederlandse Organisatie voor Wetenschappelijk Onderzoek (NWO), Netherlands; Research Council of Norway (NFR); Polish Ministry of Science and Higher Education; National Authority for Scientific Research - NASR (Autontatea Nationala pentru Cercetare Stiintifica - ANCS); Federal Agency of Science of the Ministry of Education and Science of Russian Federation, International Science and Technology Center, Russian Academy of Sciences, Russian Federal Agency of Atomic Energy, Russian Federal Agency for Science and Innovations and CERN-INTAS; Ministry of Education of Slovakia; CIEMAT, EELA, Ministerio de Educación y Ciencia of Spain, Xunta de Galicia (Consellería de Educación), CEADEN, Cubaenergía, Cuba, and IAEA (International Atomic Energy Agency); Swedish Reseach Council (VR) and Knut & Alice Wallenberg Foundation (KAW); Ukraine Ministry of Education and Science; United Kingdom Science and Technology Facilities Council (STFC); The United States Department of Energy, the United States National Science Foundation, the State of Texas, and the State of Ohio.

[1] G.C. Rossi and G. Veneziano, Nucl. Phys. **B123**, (1977) 507.

[2] A. Capella *et al.* Phys. Rep. **236**, 225 (1994); A.B. Kaidalov andK.A. Ter-Martirosyan, Sov. J. Nucl. Phys. **39**, 1545 (1984).

[3] X. Artru, Nucl. Phys. **B85**, 442 (1975); M. Imachi, S. Otsuki and F. Toyoda Prog. Theor. Phys. **52**, 341 (1974); Prog. Theor. Phys. **54**, 280 (1975).

[4] B.Z. Kopeliovich, Sov. J. Nucl. Phys. **45**, 1078 (1987); B.Z. Kopeliovich, B. Povh, Z. Phys. **C75**, 693 (1997); B.Z. Kopeliovich, B. Povh, Phys. Lett. **B446**, 321 (1999).

[5] D. Kharzeev, Phys. Lett. **B378**, 238 (1996).

[6] C. Merino *et al.* Eur.Phys.J. **C54** 577 (2008); C. Merino, M.M. Ryzhinskiy, Yu.M. Shabelski, arXiv:0906.2659.

[7] S. E. Vance and M. Gyulassy, Phys. Rev. Lett. **83**, 1735 (1999).

[8] K. Aamodt *et al.* (ALICE Collaboration), JINST **3**, S08002 (2008).

[9] K. Aamodt *et al.* (ALICE Collaboration), J. Phys. **G30**, 1517 (2004); K. Aamodt *et al.* (ALICE Collaboration), J. Phys. **G32**, 1295 (2006).

[10] P.G. Kuijer (ALICE Collaboration), Nucl. Phys. **A830** 81C (2009).

[11] R. Santoro *et al.* (ALICE Collaboration), JINST **4**, P03023 (2009); P. Christakoglou *et al.* (ALICE Collaboration), Proceedings of Science (EPS-HEP 2009) 124; K. Aamodt *et al.* (ALICE Collaboration), JINST **5**, P03003 (2010).

[12] J. Alme *et al.* (ALICE Collaboration), arXiv:1001.1950 [physics.ins-det].

[13] K. Aamodt *et al.* (ALICE Collaboration), arXiv:1004.3514; K. Aamodt *et al.* (ALICE Collaboration), arXiv:1004.3034; K. Aamodt *et al.* (ALICE Collaboration) Eur. Phys. J. **C65**, 111 (2010).

[14] W. Blum, W. Riegler and L. Rolandi, Particle Detection with Drift Chambers, 2nd ed. (Springer-Verlag, 2008).

[15] R. Brun *et al.* 1985 GEANT3 User Guide, CERN Data Handling Division DD/EE/841; R. Brun *et al.* 1994 CERN Program Library Long Write-up, W5013, GEANT Detector Description and Simulation Tool.

[16] $http://www.fluka.org/$; A. Fassó *et al.* CERN-2005-10 (2005), $INFN/TC_05/11$, SLAC-R-773; G. Battistoni *et al.* AIP Conf. Proc. **896**, 31 (2007).

[17] G. Bendiscioli and D. Kharzeev, Riv. Nuovo Cim. **17N6**, 1 (1994); R.F. Carlson, Atomic Data and Nuclear Data Tables **63** (1996).

[18] J. Kronenfeld and A. Gal, Nucl. Phys. **A430**, 525 (1984); Yu-Shun Zhang *et al.* Phys. Rev. **C54**, 332 (1996); E. Klempt *et al.* Phys. Rept. **368**, 119 (2002).

[19] T. Sjostrand, P. Skands, Eur. Phys. J. **C39**, 129 (2005); P. Skands, arXiv:1005.3457 [hep-ph] (2010), Perugia-0 (320) and Perugia-SOFT (322) tunes; A. Moraes (ATLAS Collaboration), ATLAS Note ATL-COM-PHYS-2009-119, 2009.

[20] T. Anticic *et al.* (NA49 Collaboration), Eur. Phys. J. **C65**, 9 (2010).

[21] A.M. Rossi *et al.* Nucl. Phys. **B84**, 269 (1975); M.Aguilar-Benitez *et al.* Z. Phys. **C50**, 405 (1991).

[22] B.I. Abelev *et al.* (STAR Collaboration), Phys. Rev. **C79**, 034909 (2009); I.G. Bearden *et al.* (BRAHMS Collaboration), Phys. Lett. **B607**, 42 (2005); B.B. Back *et al.* (PHOBOS Collaboration), Phys. Rev. **C71**, 021901 (2005); S. S. Adler *et al.* (PHENIX Collaboration), Phys. Rev. **C69**, 034909 (2004).

[23] A.B. Kaidalov, L.A. Ponomarev and K.A. Ter-Martirosyan, Sov. J. Nucl. Phys., **44**, 468 (1986).